COMPUTER MODELING OF COMMERCIAL REFRIGERATED WAREHOUSE FACILITIES

C. Victor Nicoulin, E.I.T., ECO Engineering
Peter C. Jacobs, P.E., Architectural Energy Corporation
Stan Tory, Pacific Gas and Electric Company

The use of computer models to simulate the energy performance of large commercial refrigeration systems typically found in food processing facilities is an area of engineering practice that has seen little development to date. Current techniques employed in predicting energy consumption by such systems have focused on temperature bin methods of analysis. Existing simulation tools such as DOE2 are designed to model commercial buildings and grocery store refrigeration systems. The HVAC and Refrigeration system performance models in these simulation tools model equipment common to commercial buildings and groceries, and respond to energy-efficiency measures likely to be applied to these building types. The applicability of traditional building energy simulation tools to model refrigerated warehouse performance and analyze energy-saving options is limited.

The paper will present the results of modeling work undertaken to evaluate energy savings resulting from incentives offered by a California utility to its Refrigerated Warehouse Program participants. The TRNSYS general-purpose transient simulation model was used to predict facility performance and estimate program savings. Custom TRNSYS components were developed to address modeling issues specific to refrigerated warehouse systems, including warehouse loading door infiltration calculations, an evaporator model, single-stage and multi-stage compressor models, evaporative condenser models, and defrost energy requirements.

The main focus of the paper will be on the modeling approach. The results from the computer simulations, along with overall program impact evaluation results, will also be presented.

INTRODUCTION

The purpose of the Refrigerated Warehouse Program is to promote the design, construction, and operation of energy efficient refrigerated warehouses and food processors. The program is designed for facilities such as new refrigerated warehouses, controlled atmosphere warehouses, food and beverage distribution centers, industrial refrigeration plants, food processing plants, refrigerated packing sheds, and wineries. Refrigeration plant expansions of new load at these facilities are also eligible.

The Refrigerated Warehouse program covers a wide variety of measures, including increased insulation levels in the building envelope, added insulation for refrigeration piping and vessels, oversized condensers, evaporator selections that raise suction temperatures and minimize fan power, improved profile compressors, quick close doors, and other facility improvements designed to improve the energy performance of refrigerated warehouse facilities and increase profits. General facility requirements, required efficiency measures, and optional measures were established by the program.

A program measurement and evaluation study[1] was conducted in 1996 in order to analyze program performance. Computer simulation was chosen as the method by which to conduct the analysis. The TRNSYS[2] general-purpose transient simulation model was used to predict facility performance and estimate program savings. Custom TRNSYS components were developed to address modeling issues specific to refrigerated warehouse systems, including warehouse loading door infiltration calculations, an evaporator model, single-stage and multi-stage compressor models, evaporative condenser models, and defrost energy requirements. Building audit reports and construction documents were obtained for eleven refrigerated warehouse facilities participating in the program evaluation study, to be used in building the computer models.

MODELING OF REFRIGERATION LOADS

Refrigeration loads are grouped into two general categories: zone loads and process loads. Refrigeration zone loads are those which exist due to heat transfer across the building envelope, air infiltration through open doorways, warm product which is introduced into a refrigerated space, and sources of heat gain from inside the refrigerated space, such as motor heat, heat from lighting, and occupant heat gains. Process loads are defined as refrigeration system loads related to operation of cooling equipment which may be located within the refrigerated space but are independent of space conditions. The magnitude of a process load will depend on the initial and final states of the product being processed, the nature of the process, and the type of process equipment used. Chilled water flumes and plate freezers are examples of process loads. Accurate simulation of refrigerated warehouse energy use and usage patterns depends on a realistic modeling of the two types of refrigeration system loads.

Zone Load Modeling

The TRNSYS Detailed Zone component was used to model each thermal zone within the warehouse facility. This component calculated space sensible and latent refrigeration loads from both zone boundary and internal sources. Loads were computed using an energy balance approach which assumed a constant space temperature and humidity ratio. The transient heat flow through each surface bounding a zone was simulated using the ASHRAE Transfer Function method. The transfer function coefficients were calculated for floors, walls, and roofs according to their construction. The detailed zone model accounted for solar radiation on opaque building surfaces and internal radiative gains by computing an equivalent inside surface temperature, which was then used to calculate the hourly heat transfer through the zone boundaries.

Zone infiltration loads were modeled using algorithms for infiltration by air exchange taken from Chapter 26 of the 1994 ASHRAE Refrigeration volume[3]. This approach accounted for heat gains resulting from room-to-room air density differences, and allowed infiltration through open doorways to be modeled as a function of the door size and type, frequency of doorway use, the doorway operation cycle length, the amount of time that the doorway remained open, and the temperature and moisture difference between the air masses in the spaces connected by the doorway. The equation used is as follows:

$$q_t = qD_tD_f(1-E) \tag{1}$$

where

q_t = average heat gain for the 24-hr or other period, Btu/h
q = sensible and latent refrigeration load for fully established flow, Btu/h
D_t = doorway open-time factor
D_f = doorway flow factor
E = effectiveness of doorway protection device

For a more detailed description of these quantities, consult the 1994 Refrigeration volume.

Hourly refrigeration loads for each product cooled by contact with zone air were calculated from the mass of product cooled, the initial and final product temperatures, and the specific heat(s) of the product. Specific heat values for food items above and below 32°F were taken from Chapter 30 of the 1993 ASHRAE Fundamentals volume[4]. Refrigeration load schedules were defined for each product. Since product cooling typically occurred over a number of hours, the schedules that were developed represented the refrigeration loads resulting from new product received during a given hour as well as the loads resulting from product received during previous hours, which would already be partially cooled at the given hour. The rate of product cooling was assumed to be constant.

In addition to shell, infiltration, and product loads, the internal heat gains from lighting, warehouse personnel, process equipment motors, forklifts or other vehicles, and evaporator coil defrosting were included as internal loads on each space. Lighting energy was split between convective and radiative load. Occupant loading was modeled using the relation for Heat Equivalent of Occupancy given in the ASHRAE Refrigeration volume.

Process equipment motor heat gain was assumed to be equal to the connected motor load. Heat gain from battery powered vehicle operation was assumed to be equal to the energy delivered to the batteries by the charging equipment.

Sensible and latent gains from defrosting of the evaporator coils were modeled using an energy balance approach based on the work of Stoecker[5] and Cole[6]. The method employed accounted for energy exchange in the form of heat and moisture gains to the conditioned space which occurred during the defrost process and energy removed with the defrost condensate. Both defrost efficiency and the proportion of heat and moisture re-entering the refrigerated space were assumed to be functions of the initial and final evaporator surface temperatures.

Once the loading on the refrigeration system from shell, infiltration, product storage, and internal gain sources was calculated, these loads were summed and imposed on the evaporators. The total hourly evaporator load was used to calculate an evaporator part load ratio, defined as the hourly zone evaporator load divided by the zone evaporator capacity. Evaporator fan heat gains were added to the zone internal heat gain, and the zone sensible and latent load equations iterated by the TRNSYS program until an energy balance was reached.

Figure 1 shows the contribution from each of the load components discussed in the preceding paragraphs to the total whole building zone load on an hourly basis for one day. The data in this figure were taken from a model of a salad processing facility. Table 1 summarizes the values of important model input parameters for this facility. Process equipment motors and defrost space gains are the most significant zone loads, followed by the envelope, product cooling, lighting, and infiltration loads. Zone loads from evaporator fan motors, occupancy, and ventilation are the least significant contributors to the zone refrigeration load. Evaporator coil defrost was turned off between the hours of 12 noon and 6 p.m., which accounts for the absence of defrost load and the drop in total load during these hours. The building was unoccupied from 2 a.m. until 6 a.m., although the lights were reportedly left on.

Figure 1. Whole Building Zone Refrigeration Loads

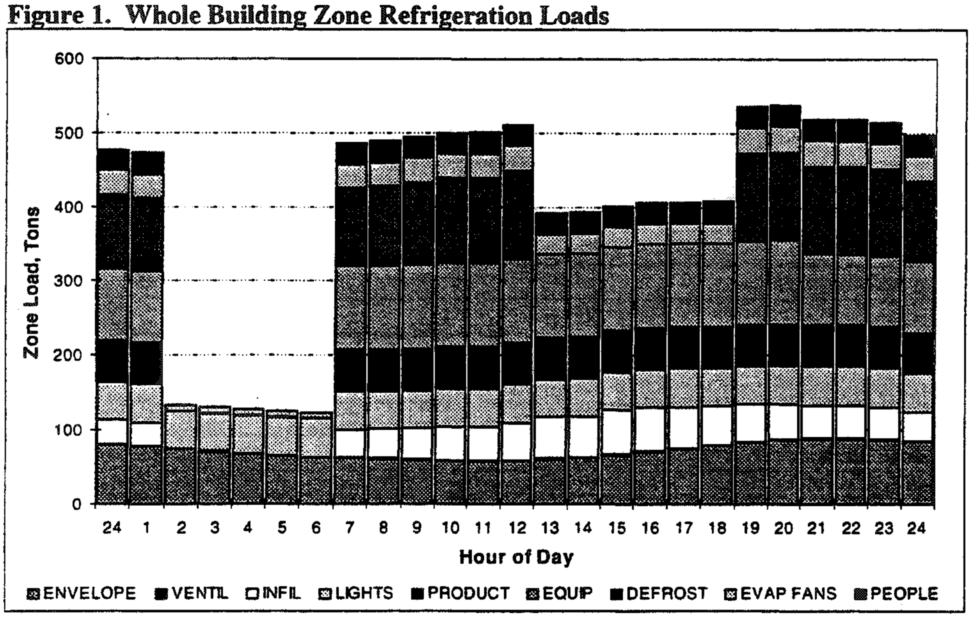

Process Load Modeling

Refrigeration system loads which resulted from process operations such as blast chilling, cooling by water immersion, or plate freezing were calculated from the mass of product being processed, the initial and final product temperatures and product specific heat(s). Process cooling loads differed from the storage cooling loads described previously in that process cooling occurred much more rapidly than storage cooling and could

Table 1. Sample Model Input Parameters

General Facility Characteristics	
Facility Type	Vegetable processing
Facility Size	172,600 square feet

Product/Process Loading

Product/Process	Lettuce	Carrots	Cauliflower	Broccoli	Spinach
Initial Temp (°F)	68	72	72	72	72
Final Temp (°F)	36	36	36	36	36

Average Daily Production by Month

Month	Lettuce (lb/day)	Carrots (lb/day)	Cauliflower (lb/day)	Broccoli (lb/day)	Spinach (lb/day)
January					240,000
February					240,000
March					240,000
April					240,000
May	500,000	50,000	50,000	50,000	240,000
June	500,000	50,000	50,000	50,000	240,000
July	500,000	50,000	50,000	50,000	240,000
August	500,000	50,000	50,000	50,000	240,000
September	500,000	50,000	50,000	50,000	240,000
October	500,000	50,000	50,000	50,000	240,000
November					240,000
December					240,000

Facility Construction and Design

Lighting		1.33 Watts/square foot
Shell Insulation	Walls	R-25
	Roof	R-35
Pipe Insulation	3-5 in. pipe	R-8.3
	6-8 in. pipe	R-11
Vessel Insulation		R-11.4
Evaporators	Capacity	1130 tons
	Fan control	One-speed
	Fan power	272 hp
	Approach temperature	8 °F
Evaporative condensers	Approach temperature	10 °F
	Min condensing temperature	60 °F
	Condenser control type	Wet-bulb control
	Fan control	Two-speed
	Fan and pump power	126 hp
Compressor plant	Efficiency (40°F zone)	0.559 bhp/ton @ 32°F suction, 78°F condensing
	Efficiency (34°F zone)	0.632 bhp/ton @ 26°F suction, 78°F condensing
	Motor efficiency	94.5%
	Oil cooling	Thermosiphon

be modeled based on product mass flow during a given hour. Product flow from previous hours did not contribute to the given (current) hour's process refrigeration loads. As with the storage refrigeration loads, schedules were defined for each process operation.

Other Refrigeration System Loads

Besides refrigeration loads from zone and process sources, refrigeration piping and vessel heat gains were included as loads on the refrigeration compressors. All of the insulated refrigerant vessels and piping runs contributing to refrigeration system loads were assumed to be located on the roof of the facility and thus were exposed to ambient temperatures. Refrigerant vessel heat gains were calculated from the overall conductance of the vessel, including insulation, and the temperature difference between the compressor suction temperature and the hourly ambient temperature:

$$Q_{vessel} = (UA)_{vessel}(T_{ambient} - T_{suction}) \tag{2}$$

Refrigerant piping heat gains were calculated based on the pipe size, insulation level, the length of each piping run for a given diameter pipe, and the temperature difference between the compressor suction temperature and the hourly ambient temperature:

$$Q_{pipe} = \frac{2\pi kL}{\ln(R_o/R_i)}(T_{ambient} - T_{suction}) \tag{3}$$

where

k = thermal conductivity of pipe insulation, Btu/hr·in·°F
L = length of pipe run in inches
R_o = radius of pipe plus insulation, in inches
R_i = radius of pipe, in inches

Piping friction losses were also included in the calculation of refrigeration plant loading. Pipe friction losses were converted to an equivalent temperature drop, based on the change in suction temperature per unit suction pressure near the suction temperature setpoint.

MODELING OF REFRIGERATION SYSTEM COMPONENTS

While it is important to accurately model system refrigeration loads, it is equally if not more important to correctly model the energy consumption by the refrigeration plant equipment. Energy consumed by compressors, condenser motors, and evaporator fans makes up the bulk of energy used by a typical refrigerated warehouse facility. Manufacturer's data were used extensively in modeling compressor and condenser performance for the variety of equipment used in large scale commercial refrigeration systems. Methods were developed which allowed the performance of the different types of refrigeration system components to be simulated with reasonable accuracy by simplified models.

Evaporators

The modeling of evaporators is potentially the most complex task of all refrigeration system component modeling efforts. Many studies have been done which analyzed coil heat transfer characteristics for modeling and analysis purposes, and the subject can become quite complex. Most of these studies did not address the effects of frost accumulation on heat transfer, coil refrigeration capacity, or refrigeration system energy consumption. Existing coil models, whether simple or complex, deal only with wet and/or dry surface conditions.

For this work it was desirable to create as simple a model as possible. Thus, coil capacity was assumed constant, and coil surface temperature assumed to be equal to the evaporator suction temperature. Individual evaporators were not modeled; instead, they were lumped into a single evaporator with a capacity equal to the total capacity of the individual units. Evaporator loads were also added together. Frost accumulation was calculated from the internal moisture gain to the space in which the evaporators were located and the humidity ratio of saturated air at the evaporator surface temperature, using a moisture balance approach.

The evaporator part load ratio mentioned previously in the discussion of evaporator fan heat gains was used to compute evaporator fan energy consumption. Depending on the fan control strategy, evaporator fan energy consumption was adjusted based on the part load ratio. For single-speed fans which ran continuously regardless of load, no adjustment was made. For single and two-speed fans that cycle on and off with load, and variable speed fans that modulate with load, the hourly fan energy was calculated as a function of part load ratio according to Figure 2.

Figure 2. Evaporator Fan Part Load Performance

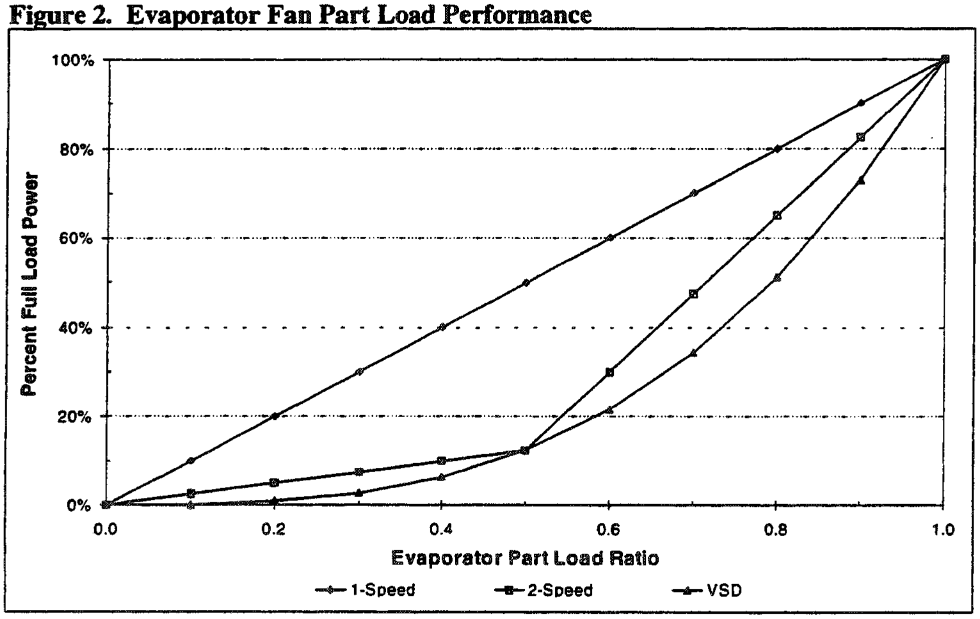

Two defrost techniques were modeled: water wash, and hot gas. Water wash defrost was assumed to have a neutral impact on facility energy use, primarily because no compressor energy was required. Also, reclaimed heat was generally available for warming the defrost make-up water. Hot gas defrost energy was computed as the energy contained in the accumulated ice divided by the defrost efficiency and the compressor COP. This energy was included as part of the compressor energy consumption for evaporators which used hot gas defrost. The final evaporator surface temperature was assumed to be identical for both water wash and hot gas defrost.

Compressors

Compressor energy use is the most significant refrigeration system end-use. The energy consumed by a refrigeration system compressor depends primarily on the suction and discharge, or condensing, temperatures under which the compressor operates. Other factors such as the type of compressor oil cooling employed affect energy use directly, while factors such as the degree of liquid subcooling and suction superheat affect the compressor capacity and therefore, for a given set of operating conditions, affect energy use in a more indirect manner. This is generally true for both single and two-stage compression systems.

Compressor performance was modeled using manufacturer's catalog data and/or compressor performance software. These data were used to create bi-quadratic regression equations which related full load compressor capacity and brake horsepower requirements to suction and condensing temperatures, as shown in the following equations:

$$TR = a_1T_s + b_1T_s^2 + c_1T_c + d_1T_c^2 + e_1T_sT_c + f_1 \tag{4}$$

$$BHP = a_2T_s + b_2T_s^2 + c_2T_c + d_2T_c^2 + e_2T_sT_c + f_2 \tag{5}$$

where

TR = full load refrigeration capacity, tons
BHP = full load compressor shaft power, horsepower
T_s = suction temperature, °F
T_c = condensing temperature, °F
$a_1 \ldots f_1$ = capacity regression coefficients
$a_2 \ldots f_2$ = shaft power regression coefficients

Suction temperature was assumed to be constant in the model, and was calculated from the temperature of the space (or final process temperature), the evaporator approach temperature (if applicable), and the suction line pressure drop (converted to temperature drop) for a given compressor circuit:

$$T_s = T_{space} - \Delta T_{approach} - \Delta T_{drop} \tag{6}$$

Correction factors for liquid injection oil cooling, liquid subcooling, and suction superheat were computed using the manufacturer's correction formulas and applied to the appropriate full load values of capacity and shaft power calculated by the regression equations.

The corrected full load capacity is the total refrigeration effect that the compressor can supply at a given set of suction and condensing conditions, and the shaft power is the compressor energy input required to achieve the total refrigeration effect. Compressors run at full load only a fraction of the 8760 hours in each year. As the loads imposed on each compressor decrease, the compressors employ various unloading techniques to reduce their refrigeration capacity in order to match their loading. The effect of the capacity control devices on compressor energy use was calculated using a part load adjustment factor. The adjustment factor is a function of compressor suction temperature and the compressor part load ratio. Manufacturers catalog data were used to develop the part load adjustment factors. Curves representing the catalog data were regressed using a bi-quadratic equation form. Figure 3 shows the regression curves thus obtained. For a given compressor suction

Figure 3. Compressor Part Load Correction Curves

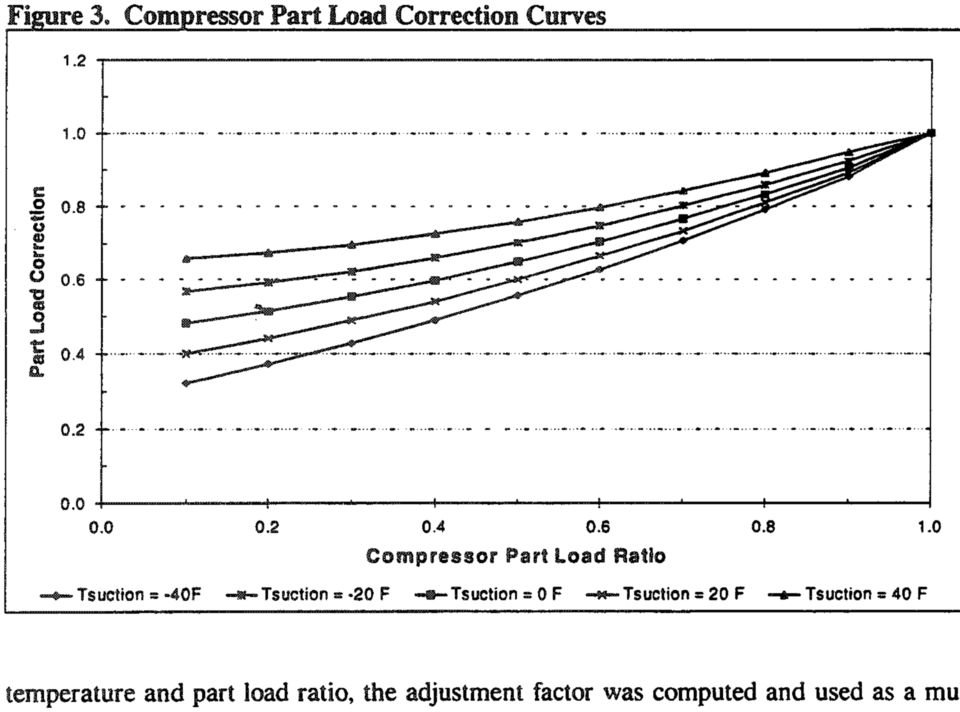

temperature and part load ratio, the adjustment factor was computed and used as a multiplier to the full load compressor shaft power. Compressor part load ratio was defined as the hourly compressor load divided by the corrected full-load compressor capacity.

In addition to compressor capacity control devices that are internal to the compressors, staging of individual compressors was modeled by creating schedules which emulated the behavior of real compressor staging control. The foreknowledge of compressor loading greatly facilitated this approach, which would have been made considerably more complex if the refrigerated warehouse model was designed for a forecasting application.

Condensers

The condensers that were modeled were exclusively evaporative condensers, although the algorithms that were developed could easily be modified to simulate the heat rejection and energy performance of dry condensers. Condensing performance, in terms of heat rejection rate and motor energy consumed by fans and pumps, is a function of condensing temperature, ambient wet bulb temperature, and the condenser part-load ratio. The condenser performance was modeled based on the heat rejection rate of the condenser at standard conditions and an adjustment factor (sometimes called an oversizing factor) based on condensing temperature and wet bulb temperature. The algorithm follows closely the Heat of Rejection condenser sizing method published in the condenser manufacturers' literature[7].

As with the compressor model, manufacturers' catalog data were used to develop a bi-quadratic regression model of the condenser heat rejection adjustment factor as a function of condensing temperature and wet bulb temperature. The heat rejection factor curves obtained from regression of manufacturers' tabular heat rejection factor data are shown in Figure 4.

Figure 4. Condenser Heat Rejection Factor Curves

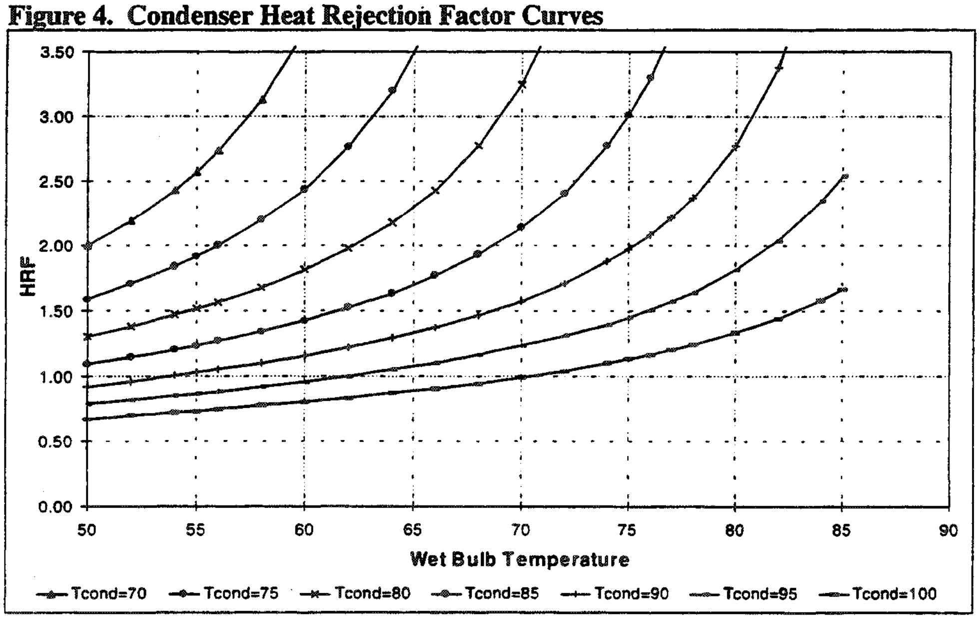

The hourly condensing temperature is a function of the heat rejection capacity of the condenser, the load imposed on the condenser by the compressor plant, and the condensing temperature control strategy employed. Two types of condensing temperature control strategies were modeled: pressure control and wet bulb control. In pressure control the condenser fans run at full speed, thus maximizing the heat rejection rate of the condenser and minimizing condensing temperature. As the condensing temperature approaches the minimum condensing temperature setpoint (the floating head pressure setpoint), the condenser fan operation, and thus the condenser air flow rate, is controlled to maintain the condensing temperature at the minimum condenser temperature setpoint.

In wet bulb control, the condenser fan operation and air flow rate are controlled to maintain a fixed difference between the condensing temperature and the wet bulb temperature. If the condensing temperature is above the fixed differential, the fans run at full speed and air flow is at the maximum. As the condensing temperature approaches the condensing temperature setpoint, the condenser fans begin to cycle and air flow rate is modulated to maintain the fixed differential. As with pressure control, condenser fan operation and air flow rate are also controlled to maintain the condensing temperature at the minimum condensing temperature setpoint (corresponding to the floating head pressure setpoint).

The modeling approach for the simulation of condensers with pressure control was to compare the heat rejection capacity of the condenser at given wet bulb and condensing temperatures with the total heat rejected by the compressor plant. The condensing temperature was recalculated in an iterative process until the heat rejection rate of the condenser equaled the total heat rejected by the compressor plant If the calculated condensing temperature was less than the minimum condensing temperature, the condensing temperature was fixed at the minimum value and the condenser fans were allowed to cycle off.

In contrast, the modeling approach for simulating condensers with wet bulb control was to calculate a condensing temperature setpoint equal to the wet bulb temperature plus the condenser approach temperature. If the heat rejection rate of the condenser at this setpoint was less than the total heat rejected by the compressor plant, the condensing temperature was allowed to float above the setpoint until the heat rejection rates were equal. If, at the condensing temperature setpoint, the heat rejection capacity of the condenser was greater than the total heat rejected, the condensing temperature was fixed at the setpoint and the condenser fan operation was modulated.

Individual condenser fans were modeled as a single fan with a horsepower rating equal to the sum of the individual motor ratings. Condenser fan energy was calculated based on the condenser part-load ratio and the type of fan arrangement employed. The condenser part-load ratio was defined as the hourly heat rejection by the compressor plant divided by the condenser heat rejection capacity at the current hour's conditions. This definition is analogous to the definitions for evaporator and compressor part-load ratios given previously. Condenser fan energy was calculated according to the part-load performance curves shown in Figure 5. Note

Figure 5. Condenser Fan Part-Load Performance Curves

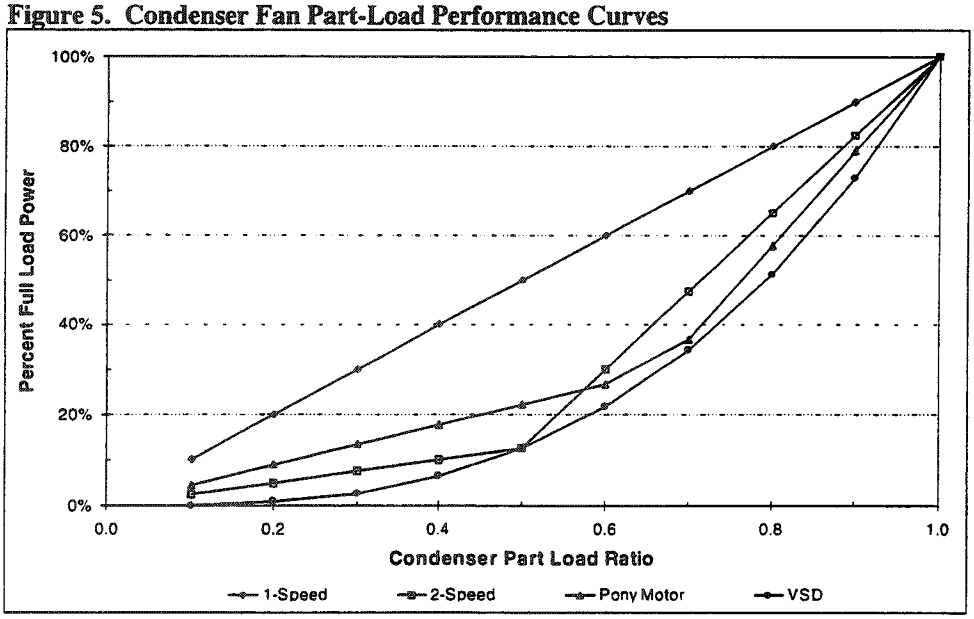

that condenser capacity was assumed to vary as shown in the Figure for the various fan arrangements down to a part-load ratio of 0.10. Below this point, heat rejection from the condenser was assumed to occur via natural convection and fan energy was zero. Condenser pump motors were modeled as a single motor with a rating equal to the sum of the individual pump motors as well, and were assumed to run continuously.

CALIBRATED MODEL RESULTS

The results of the models of several sites were compared to billing data collected during the 1995 calendar year. Sites for calibration were selected based on the completeness of the billing data, and the match between the modeled space and the space served by the meter(s). Monitored weather data for 1995 were used to drive the calibration simulations.

Of the three sites for which the match between the metered space and the modeled space permitted calibration, two were successfully calibrated and the third calibrated reasonably well. Figure 6 shows the results of calibration to monthly electrical energy consumption for the example salad processing facility referenced previously in this paper. Figure 7 illustrates the comparison between calibrated model demand and monthly billing demand for the same facility.

Figure 6. Comparison of Simulated to Actual Electrical Energy Use

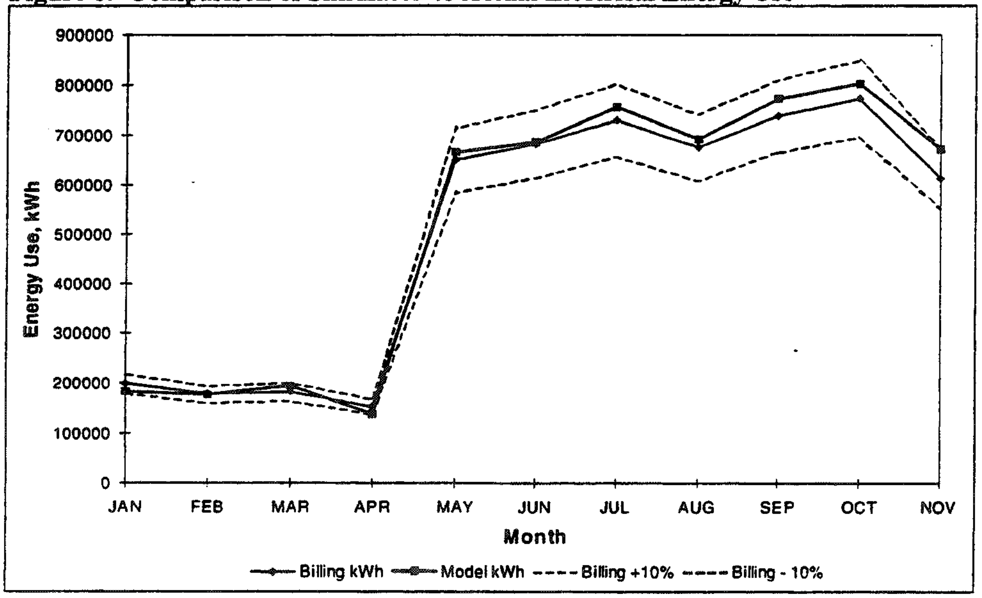

Figure 7. Comparison of Simulated to Actual Electric Demand

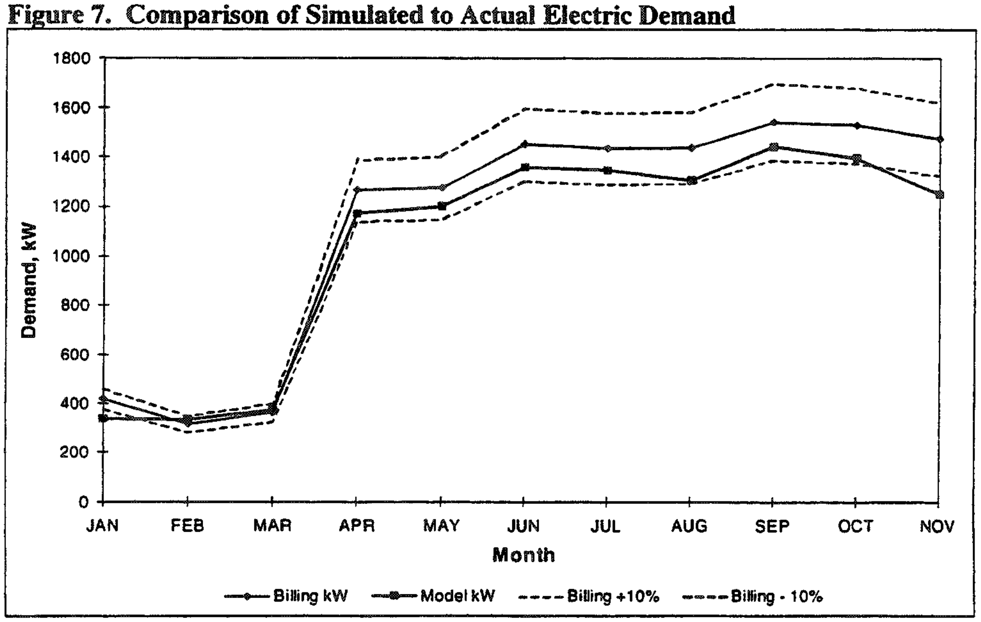

PROGRAM IMPACT EVALUATION RESULTS

Annual gross energy savings estimates for the eleven program participants is shown in Table 2. Gross savings are calculated simply as the difference in annual energy consumption between a building incorporating program incentive measures and a baseline building which was constructed according to the program definition of standard practice. Summer peak demand savings are shown in Table 3. Along with the estimated savings computed from simulation results, the expected savings from program incentive calculations is shown. The realization rate on gross savings is simply the estimated savings divided by the program expected savings.

Table 2. Annual kWh Savings by Site

Site Number	Condenser	Compressor	Evaporator	Total Estimated	Program Expected	Realization Rate
1	6,910	2,501,144	374,298	2,882,752	3,049,196	0.945
2	43,270	1,956,380	207,220	2,208,288	1,356,064	1.628
3	-23,420	248,341	128,767	353,835	952,490	0.371
4	68,645	2,625,692	409,286	3,103,618	2,649,940	1.171
5	30,046	315,459	42,873	388,750	1,051,024	0.370
6	9,055	406,540	291,674	707,285	253,298	2.792
7	-387,241	1,461,619	41,860	1,118,219	2,854,146	0.392
8	-2,567	756,019	2,925	757,319	510,594	1.483
9	-124,222	891,994	0	768,490	1,443,035	0.533
10	-20,816	583,862	277,170	840,140	580,402	1.448
11	-12,560	174,807	41,133	203,316	115,341	1.763
Total				13,332,011	14,815,530	0.900

Table 3. Summer Peak kW Savings by Site

Site Number	Condenser	Compressor	Evaporator	Total Estimated	Program Expected	Realization Rate
1	-8	442	112	530	426	1.244
2	6	435	53	500	256	1.953
3	-2	146	66	210	123	1.707
4	-12	564	112	630	335	1.881
5	8	214	27	248	185	1.341
6	1	61	10	76	19	4.000
7	-111	403	12	310	526	0.589
8	-1	190	1	191	93	2.054
9	-37	285	0	243	215	1.130
10	-8	68	26	80	90	0.889
11	-2	21	6	26	14	1.850
Total				3,044	2,282	1.334

Overall, the program achieved approximately 90 percent of the expected kWh savings and 133 percent of the expected demand savings. The site-by-site kWh realization rates varied from a minimum of 0.37 to a maximum of 2.8. Similarly, the realization rates for summer peak demand savings varied from a minimum of 0.59 to a maximum of 4.0.

The wide variability in the site-by-site realization rates arose from several factors. A key assumption in the development of savings estimates was the annual facility utilization, as expressed in terms of the annual full load hours. The annual full load hours was defined as the total annual refrigeration load (in ton-hours) divided by the total compressor plant capacity at design conditions (in tons). The savings estimates were based on full load hours that were consistent with year-round, 24 hour per day operations. Many of the participating facilities were operated less than 24 hours per day, and several experienced distinct seasonal fluctuation in their operation. Seasonal operations in particular resulted in low utilization of the refrigeration equipment and lower realization rates. In general, the realization rates for facilities that were well-designed and reasonably loaded exceeded unity, indicating that the program savings calculations were conservative.

Also, the gross savings were calculated for both incented and non-incented measures. Several energy efficiency strategies were incorporated into program minimum specifications which paid no incentives and were not included in the program savings estimates, such as reduced lighting levels. Also, several program participants adopted energy efficiency strategies that were not given incentives under the program.

The negative savings associated with condenser fans and pumps was generally expected, since the oversized condensers required by the program typically consume more fan and pump energy to achieve lower approach temperatures. The oversized condensers improve the efficiency of the compressor plant, resulting in positive combined compressor and condenser savings. Positive condenser savings were obtained for sites where fan and pump motor substitutions reduced the motor horsepower to near the baseline levels specified by the program.

Five program participants refused to participate in the evaluation. Since the full census of participants was not studied, the gross realization rate for the sites studied was applied to the savings for program participants who refused involvement in the evaluation study. The adjusted savings for each of the refusing customers was then allocated across each end-use an costing period. Table 3 shows the gross program impacts by costing period. The net program savings, including all participants, are shown in Table 4. Net savings were calculated by adopting a default 0.75 net to gross.

Table 3. Gross Program Savings by Costing Period

Costing Period	Average kW Savings	Annual kWh Savings
Summer On Peak	3,335	1,994,431
Summer Partial Peak	3,053	1,981,536
Summer Off Peak	3,267	4,518,708
Winter Partial Peak	2,510	2,737,589
Winter Off Peak	2,531	3,620,115

Table 4. Net Program Savings by Costing Period

Costing Period	Average kW Savings	Annual kWh Savings
Summer On Peak	2,501	1,495,823
Summer Partial Peak	2,290	1,486,152
Summer Off Peak	2,450	3,389,031
Winter Partial Peak	1,882	2,053,192
Winter Off Peak	1,898	2,715,087

CONCLUSIONS

Given the task of creating a simplified computer model to evaluate the energy performance of refrigerated warehouses, the engineering algorithms employed in the TRNSYS model successfully simulated the energy performance of the warehouse facilities participating in the evaluation study. The model calibrated reasonably well to utility billing data for the facilities where the meter data matched the modeled area. The savings estimated by simulation were generally comparable to the program's expected savings estimates. Where the simulation results diverged from expected values, the deviations were due to differences in the assumptions which defined facility loading and operation.

The evaluation study performed was limited in the sense that the impact analysis examined the cumulative effects of the individual program measures employed at each participating facility, rather than examining program measure impacts on a measure-by-measure basis. A measure-by measure analysis would not only refine the evaluation results in such a way that the effectiveness of individual measures could be assessed, but would also allow the various engineering algorithms to be tested and refined as well. Further modeling efforts should be directed at this type of analysis.

The general engineering knowledge of actual facility loading and operation characteristics in refrigerated warehouses may be expanded by further study of product loading, process equipment loading and operation, refrigeration plant component loading and operation, and refrigeration system controls. Research of this type would be well supported by short and long-term monitoring of process and plant equipment by data logging devices or DDC control system data. Product loading studies should address issues such as seasonal variation in field heat and bulk cooling rates.

REFERENCES

1. Measurement and Evaluation Program, Customer Energy Efficiency Policy & Evaluation Section. 1997. *Impact Evaluation of Pacific Gas & Electric Company and Southern California Edison 1994 Nonresidential New Construction Programs–PG&E Study Number 323 (SCE Study Number 522).* San Francisco, California: Pacific Gas and Electric Company.

2. Solar Energy Laboratory. 1990. *TRNSYS - A Transient Systems Simulation Program - User's Manual.* Engineering Experiment Station Report No. 38-13. Madison, Wisconsin: University of Wisconsin.

3. ASHRAE. 1994. *Refrigeration Systems and Applications Handbook.* Atlanta, Georgia: American Society of Heating, Refrigerating, and Air-Conditioning Engineers, Inc.

4. ASHRAE. 1993. *Fundamentals Handbook.* Atlanta, Georgia: American Society of Heating, Refrigerating, and Air-Conditioning Engineers, Inc.

5. Stoecker, W. F., J. J. Lux, Jr., and R. J. Kooy. 1983. "Energy Considerations in Hot-Gas Defrosting of Industrial Refrigeration Coils". *ASHRAE Transactions*, Volume 89, Part 2a. Atlanta, Georgia: American Society of Heating, Refrigerating, and Air-Conditioning Engineers, Inc.

6. Cole, R. A. 1989. "Refrigeration Loads in a Freezer Due to Hot Gas Defrost and Their Associated Costs". *ASHRAE Transactions*, Volume 95, Part 2. Atlanta, Georgia: American Society of Heating, Ventilating, and Air-Conditioning Engineers, Inc.

7. EVAPCO, Inc. 1991. *Bulletin 150B–ATC Evaporative Condensers.* Westminster, Maryland: EVAPCO, Incorporated.